Proceedings of the 4th International Conference on Biological Engineering and Medical Science
DOI: 10.54254/2753-8818/64/2024.18001

Target-based drug repositioning in papillary renal cell carcinoma with TFE3 fusion

Sungjoo Han[1,†], Sejoon Lee[2,3,†], Jae Won Yun[4,5,*], Soyeon Ahn[1,6,*]

[1]Medical Research Collaborating Center, Seoul National University Bundang Hospital, Seongnam, Korea
[2]Precision Medicine Center, Seoul National University Bundang Hospital, Seongnam, Korea
[3]Department of Pathology and Translational Medicine, Seoul National University Bundang Hospital, Seongnam, Korea
[4]Veterans Medical Research Institute, Veterans Health Service Medical Center, Seoul, Korea

[5]jwyunmd@gmail.com
[6]ahnsoyeon@snubh.org
*corresponding author
[†]These authors contributed equally to this work.

Abstract. Papillary renal cell carcinoma (PRCC) is the second most common subtype of renal cell carcinoma. Recurrent transcription factor E3 (*TFE3*) fusions have been identified in PRCC. Although patients with *TFE3* fusions show relatively aggressive phenotypes, no effective targeted therapies have been developed. In this study, we aimed to identify putative therapeutic targets through systematic bioinformatic analysis of PRCC with *TFE3* fusion. We identified *TFE3* fusion cases (n = 6) and controls (n = 282) in The Cancer Genome Atlas database. A total of 1,314 differentially expressed genes were extracted. An overrepresentation analysis revealed cancer-related signaling pathways, which were categorized to 13 cancer-related pathways, including nuclear factor-erythroid factor 2-related factor 2 (NRF2)-, G protein-coupled receptor (GPCR) signaling-, inflammatory response-, development-, and insulin-like growth factor-related pathways. A network analysis and literature review were performed using drug-target databases to identify putative applicable drugs. We identified several promising drug candidates for PRCC with *TFE3* fusion, including amrubicin, *BCL6* inhibitors (79-6, BI-3812), cetuximab, epirubicin, gemcitabine, ipilimumab, linsitinib, olaparib, Orencia®, paclitaxel, panitumumab, sorafenib, and tamoxifen. Our suggested strategy can help bridge the gap between transcriptome studies and the choice of therapeutic agents. Further experimental validation is needed to improve the efficacy of precision medicine for PRCC.

Keywords: biomarker, drug repositioning, papillary renal cell carcinoma, pathway analysis, RNA-Seq, *TFE3* fusion.

DOI: 10.54254/2753-8818/64/2024.18001

1. Introduction

Renal cell carcinoma (RCC) accounts for approximately 85% of kidney cancers and accounts for the highest mortality rate among genitourinary cancers [1-3]. RCC comprises multiple heterogeneous cancer types [3], with papillary renal cell carcinoma (PRCC) being the second most common subtype, accounting for 15%–20% of RCC [4]. Approximately 1%–4% of patients with RCC have gene fusions involving transcription factor E3 (*TFE3*) in Xp11.2; most of these patients show relatively aggressive phenotypes and a papillary pattern [4-8]. However, the molecular biology underlying *TFE3* fusions in PRCC remains largely uncharacterized, and effective targeted therapies have not yet been identified [9].

According to the National Comprehensive Cancer Network guidelines, there are no specific therapeutic agents for *TFE3* fusion-positive PRCC, and only data of phase II clinical trials on sunitinib and everolimus in patients with non-clear cell RCC, including cases with Xp11.2 translocation, have been reported with limited statistical value [10]. Thus, there is an urgent clinical need to identify candidate drugs for *TFE3* fusion-positive cancers.

Drug repositioning is a cost-effective strategy for developing unknown treatment options [11]. In this study, we aimed to identify potential therapeutic targets for *TFE3* fusion-positive PRCC through a systematic bioinformatic analysis. By analyzing gene expression data and describing the transcriptomic features and signaling pathways specific to PRCC with *TFE3* fusion, we suggested putative actionable drugs and targets can be repurposed for the treatment of this aggressive cancer subtype.

2. Materials and methods

2.1. Data acquisition and pre-processing

The RSEM-normalized *TFE3* mRNA expression data were downloaded from the cBioPortal website (https://www.cbioportal.org). The Cancer Genome Atlas (TCGA) kidney renal papillary cell carcinoma (KIRP) RNA-Seq data and clinical information of 321 patients aligned to the hg19 reference genome were downloaded from the GDC Data Portal (https://portal.gdc.cancer.gov). The raw count data had 34,180 Ensembl gene IDs, 11,758 (34%) of which were converted to Entrez IDs using ensemblDB. Patients with primary solid tumor samples identified by TCGA barcode 01 (288 patients, 11,758 gene IDs) were included in the main analysis.

2.2. Case-control setting

Six *TFE3* fusion-positive samples from TCGA KIRP were identified from the TumorFusions web data portal (https://tumorfusions.org). Compared to non-fusion-positive cases, *TFE3* fusion-positive cases showed higher mean ± SD *TFE3* expression z-scores (–0.018 ± 0.969 vs. 1.003 ± 1.832). Fifty percent of the non-fusion-positive cases with the lowest expression value of *TFE3* were set as controls (n = 140). (Survival rates varied between the *TFE3* fusion-positive cases and controls (log-rank test $p < 0.001$, figure 2, figure A1). To avoid noise from certain samples, we randomly selected 70 samples from the controls; this process was repeated 100 times (figure 1).

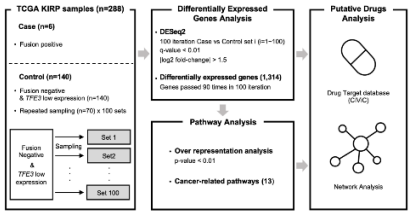

Figure 1. Overall workflow of this study. We used RNA-Seq data from The Cancer Genome Atlas (TCGA) Kidney renal papillary cell carcinoma (KIRP) database and identified 1,314 differentially expressed genes (DEGs, q-value < 0.01, $\log_2$ fold-change > 1.5) in *TFE3* fusion-positive papillary renal cell carcinoma (PRCC). A total of 13 major cancer-related pathways were identified using overrepresentation analysis. Putative drugs were determined using a drug-target database and visualized in a drug-target network analysis.

DOI: 10.54254/2753-8818/64/2024.18001

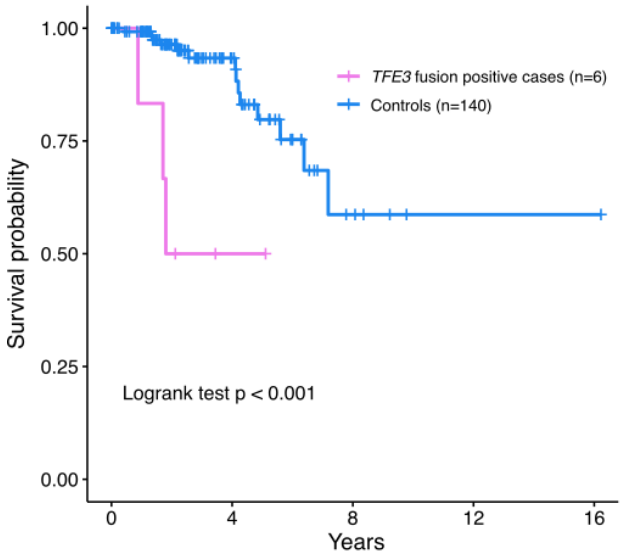

Figure 2. Kaplan–Meier curves for *TFE3* fusion-positive cases (n = 6) and controls (n = 140). The plot represents the difference in survival rate between the groups ($p < 0.001$).

2.3. Differentially expressed gene (DEG) analysis

DEG analysis was performed 100 times with different controls each time, using DESeq2. DEGs were selected with q-value and $\log_2$ fold-change cutoff values of 0.01 and 1.5, respectively. A total of 2,019 and 1,606 genes were upregulated and downregulated, respectively. DEGs that appeared more than 90 times during the 100 permutations were selected (figure A2). A total of 1,314 DEGs were selected, comprising 576 upregulated and 738 downregulated genes. Cancer-related DEGs were identified in a publicly available database, the Bushman lab [12].

2.4. Pathway analysis

Clinical summary data were obtained from the Clinical Interpretations of Variants in Cancer (CIViC) [13]. A total of 1,314 DEGs were matched to the CIViC data.

2.5. Statistical analysis and visualization

All statistical analyses were performed using R version 3.12 software (The R Foundation, Vienna, Austria). An RNA expression heatmap with the related pathways was visualized using ComplexHeatmap. A network between related pathways and targetable drugs was visualized using Cytoscape software (The National Institute of General Medical Sciences, USA).

3. Results

3.1. Clinical and pathological characteristics

Clinical and pathological characteristics were compared between *TFE3* fusion-positive cases and controls among patients with PRCC in TCGA-KIRP (table 1). Significant differences were observed between these groups in the vital status and tumor stage, whereas age, sex, and mutation profile did not differ significantly.

Mortality rate was higher in the *TFE3* fusion-positive cases than in the controls (50% vs. 10%, chi-squared test $p < 0.05$). The survival curves were significantly different between the *TFE3* fusion-positive cases and controls (log-rank test $p < 0.01$, figure 2), as well as between the *TFE3*-high expression and control groups ($p < 0.01$, figure A1).

DOI: 10.54254/2753-8818/64/2024.18001

TFE3 fusion-positive cases were associated with advanced tumor stages. The dominant stages in the *TFE3* fusion-positive cases and controls were stage 3 (66.7%) and stage 1 (70%), respectively (p = 0.002).

Table 1. Clinical and pathological characteristics of *TFE3* fusion-positive cases and controls.

	Total (n = 146)	**Fusion positive (n = 6)**	**Controls (n = 140)**	**p**
Age (years), median (range)	61.3 (28–85)	52.8 (37–64)	61.7 (28–85)	0.063
Sex				0.089
Male	122 (83.6%)	3 (50.0%)	119 (85.0%)	
Female	24 (16.4%)	3 (50.0%)	21 (15.0%)	
Vital status				0.019
Alive	129 (88.4%)	3 (50.0%)	126 (90.0%)	
Dead	17 (11.6%)	3 (50.0%)	14 (10.0%)	
Stage				0.002
Stage I	100 (68.5%)	2 (33.3%)	98 (70.0%)	
Stage II	11 (7.5%)	0 (0.0%)	11 (7.9%)	
Stage III	18 (12.3%)	4 (66.7%)	14 (10.0%)	
Stage IV	3 (2.1%)	0 (0.0%)	3 (2.1%)	
Unidentified	14 (9.6%)	0 (0.0%)	14 (10.0%)	
Mutation[†]				
MET	15 (10.8%)	0 (0.0%)	15 (11.3%)	0.843
FAT1	3 (2.2%)	0 (0.0%)	3 (2.3%)	> 0.999
NF2	2 (1.4%)	0 (0.0%)	2 (1.5%)	> 0.999
BAP1	4 (2.9%)	0 (0.0%)	4 (3.0%)	> 0.999
PBRM1	2 (1.4%)	0 (0.0%)	2 (1.5%)	> 0.999
SMARCB1	2 (1.4%)	0 (0.0%)	2 (1.5%)	> 0.999
STAG2	2 (1.4%)	0 (0.0%)	2 (1.5%)	> 0.999
TP53	2 (1.4%)	0 (0.0%)	2 (1.5%)	> 0.999
KDM6A	5 (3.6%)	0 (0.0%)	5 (3.8%)	> 0.999
SETD2/NFE2L2	0 (0.0%)	0 (0.0%)	0 (0.0%)	> 0.999

[†] Data of 139 mutation samples (6 *TFE3* fusion-positive cases and 133 controls) were available.

3.2. DEGs and pathways

We initially identified 91 pathways in the confirmed 1,314 DEGs by overrepresentation of ConsensusPathDB ($p < 0.01$). We manually curated 13 cancer-related pathways, which included 39 pathways and 155 associated DEGs (table B1).

Heatmap visualization revealed the following cancer-related pathways based on the expression value of DEGs: nuclear factor-erythroid factor 2-related factor 2 (NRF2)-, G protein-coupled receptor (GPCR) signaling-, inflammatory response-, development-, insulin-like growth factor-, axon guidance-, steroid synthesis-, cell cycle-, differentiation-, nicotine metabolism-, cell–cell junction-, extracellular matrix-, and integrin-related pathways (figure 3, figure A3). Among the 10 genes with the lowest p-values in the cancer-related pathways, 6 genes were upregulated (*DLL1*, *SCARB1*, *FN1*, *CTSK*, *SQSTM1*, and *NCAM1*) and 4 were downregulated (*KRT7*, *EPHA1*, *SLC6A20*, and *CD24*).

The network analysis revealed key genes involved in various pathway groups (figure 4). *FN1* was involved in five pathways, including axon guidance-, development-, extracellular matrix-, and inflammatory response-related pathways (figure 4, diamond node). *COL4A1*, *COL6A3*, *ITGA1*, *KITLG*, and *LAMC2* were related to four pathways, three of which were involved in axon guidance-,

DOI: 10.54254/2753-8818/64/2024.18001

development-, extracellular matrix-, and integrin-related pathways (figure 4, triangle nodes). *CDH1*, *COL1A1*, *COL3A1*, *EREG*, *FGF9*, *ITGB4*, *NCAM1*, *RASGRF1*, *SHH*, *THBS1*, *UGT1A9*, and *VTN* were related to three pathways (figure 4, square nodes). The 45 genes were involved in two pathways. Only the insulin-like growth factor-related pathway clustered exclusively.

We identified 136 cancer-related genes among the 1,314 DEGs using the Bushman lab database (table B2). The gene most extensively related to multiple pathways, *FN1*, was cancer-related. In addition, *FN1* had the second highest fold change value (4.89) among the cancer-related-DEGs (details in the Discussion). *ITGA* and *KITLG* were cancer-related genes among the five genes linked to four pathways (figure 4, triangle nodes). Among the 12 genes involved in three pathways, the cancer-related genes were *CDH1*, *COL1A1*, *COL3A1*, *FGF9*, *ITGB4*, *RASGRF1*, *SHH*, and *THBS1* (figure 4, square nodes).

3.3. Elucidation of targeted drugs

Based on the CIViC database and a literature review, we identified putative actionable drugs targeting either DEGs or cancer-related pathways. A total of 14 putative drugs were confirmed to target 11 DEGs: Orencia® and ipilimumab for *CD80*, linsitinib for *IGF2BP3*, epirubicin for *FOXP3*, paclitaxel for *PDCD4*, cetuximab and panitumumab for *EREG*, *BCL6* inhibitors (79-6, BI-3812) for *BCL6*, amrubicin for *NQO1*, gemcitabine for *MAGEH1*, olaparib for *CBLC*, tamoxifen for *AGR2*, and sorafenib for *PROM1*.

The drugs were divided into two groups according to their clinical significance, and the target genes involved in multiple pathways were identified. For example, *NQO1* was associated with the NRF2-related and steroid synthesis-related pathways, and amrubicin was the target drug (figure 5). *EREG* was involved in GPCR signaling-, development-, and axon guidance-related pathways and had two putative drugs, cetuximab and panitumumab.

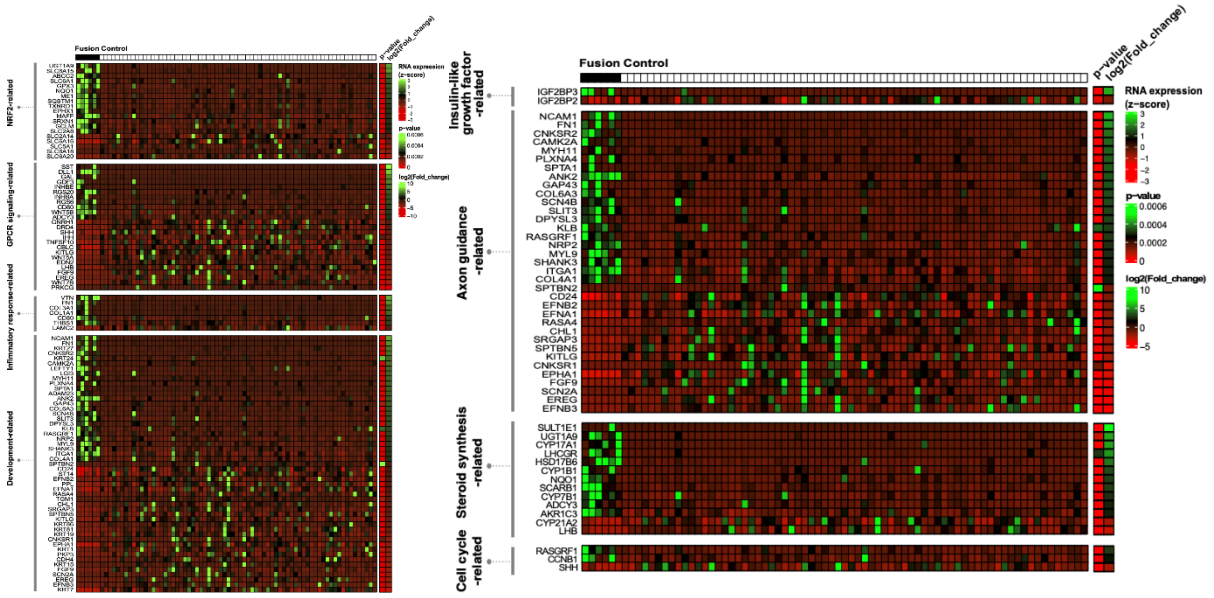

Figure 3. Gene expression heatmap of cancer-related pathways. A total of 150 DEGs were associated with nuclear factor-erythroid factor 2-related factor 2 (NRF2)-, G protein coupled receptors (GPCR) signaling-, inflammatory response-, development-, insulin-like growth factor-, axon guidance-, steroid synthesis-, and cell cycle-related pathways. Pathways with $p < 0.01$ were selected and merged based on pathway ontology. RNA expression was converted to the z-scores presented in the heatmap.

DOI: 10.54254/2753-8818/64/2024.18001

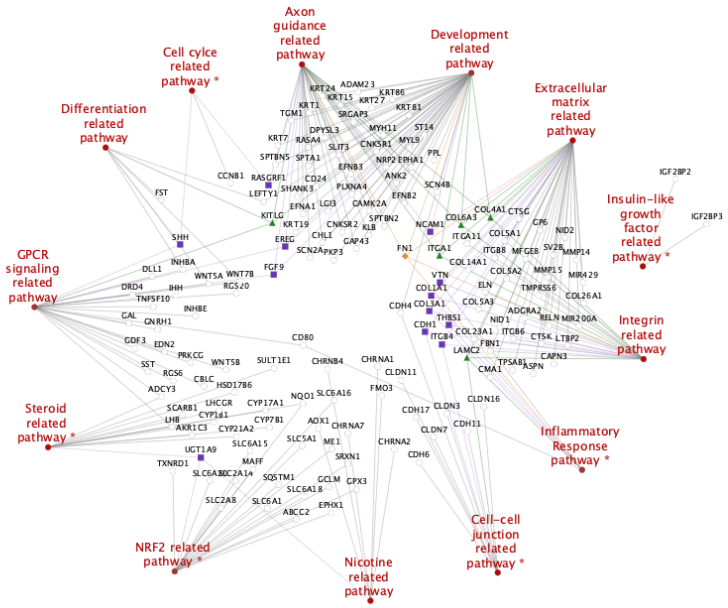

Figure 4. Differentially expressed genes (DEGs) involved in cancer-related pathways of *TFE3* fusion-positive cases. Pathways and associated DEGs are connected to the edges. The 13 cancer-related pathways are positioned outside the circle and the related DEGs are indicated in black font. Some genes involved in multiple pathways are indicated in diamond (five pathways), triangle (four pathways), and square (three pathways).
* Pathways known to be related to *TFE3* from previous research.

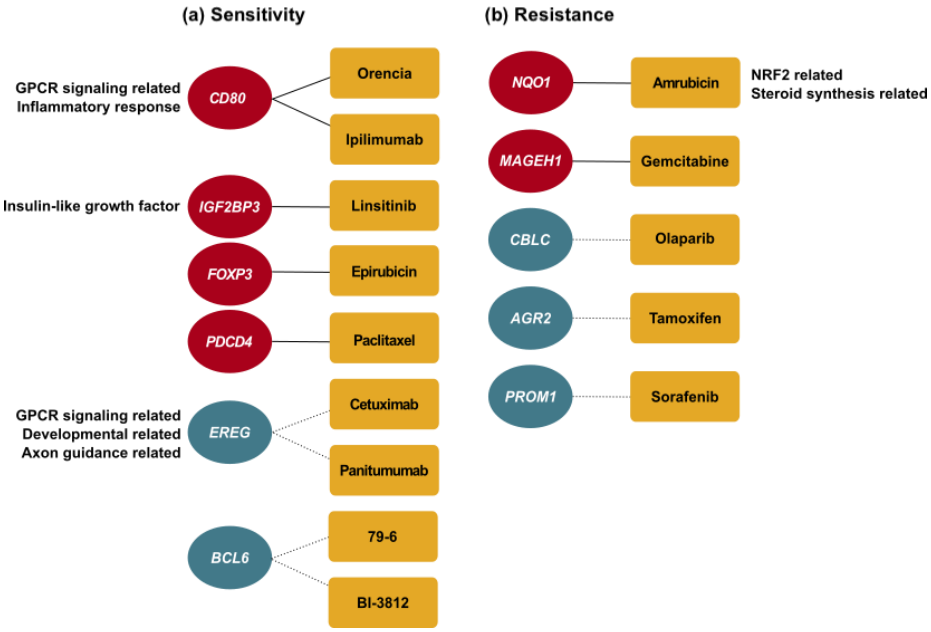

Figure 5. Drug-target network of *TFE3* fusion-positive cases. (a) Drugs with putative sensitivity. (b) Drugs with putative resistance. Oval: genes; rectangle: target drugs; solid line: over-expressed genes in *TFE3* fusion-positive cases, related with at least one type of cancer in the Clinical Interpretations of Variants in Cancer database or other literature; dotted line: underexpressed genes, reported in the literature but with inconsistent gene expression levels compared with the findings of the present study.

DOI: 10.54254/2753-8818/64/2024.18001

4. Discussion

Herein, we described downstream pathways of downregulated gene in *TFE3* fusion-positive PRCC based on a systematic computational method. This is the first study to systematically determine putative target drugs for *TFE3* fusion PRCC.

PRCC patients with *TFE3* fusion are treated with conventional chemotherapy, which is not specific to the *TFE3* fusion type. Some conventional treatments for PRCC include tyrosine kinase inhibitors with a VEGF inhibition mechanism (i.e., cabozantinib, sunitinib, lenvatinib with everolimus, axitinib, and bevacizumab) [14]. Our study suggests that cetuximab, panitumumab, and sorafenib function as tyrosine kinase inhibitors. Sorafenib is the standard treatment for clear RCC, and it involves the VEGF inhibitor mechanism. However, VEGF inhibitors should be considered in non-clear cell RCC because of its low response rate and high risk of progression [15].

Our analyses also revealed putative drugs that use a mechanism different from that of tyrosine kinase inhibitors, such as amrubicin, olaparib, paclitaxel, tamoxifen, epirubicin, *BCL6* inhibitors (79-6, BI-3812), Orencia®, ipilimumab, and gemcitabine. We first grouped the drugs based on their biological mechanisms, for example: amrubicin, epirubicin, and gemcitabine inhibit the DNA replication mechanism, followed by cell growth inhibition and cell death; ipilimumab and Orencia® interact with T lymphocytes, thereby reducing their activity.

We also categorized drugs that would regulate either sensitivity or resistance when the target gene is overexpressed. Drugs related to overexpressed genes in *TFE3* fusion-positive cases were related to at least one type of cancer in the CIViC database or other literature (figure 5, solid lines). The second grouping of drugs was related to underexpressed genes, although the gene expression levels in our study were not consistent with the reported findings. Therefore, we inferred that the second group of drugs was more likely to be effective in non-fusion-positive PRCC (figure 5, dotted lines). Thus, we strongly suggest the first group of drugs, including Orencia®, ipilimumab, linsitinib, epirubicin, and paclitaxel, to be subjected to further investigation.

The suggested drugs exhibit anti-cancer effects on *TFE3* fusion-positive cells (figure 5, solid lines). Drugs related to underexpressed genes in *TFE3* fusion-positive patients are more likely to affect non-fusion-positive patients, as the drugs exert adverse effects when target genes are overexpressed (figure 5, dotted lines).

Some cancer-related pathways inferred in this study are consistent with those reported previously. First, the *NRF2* pathway is a distinguishing feature of type 2 PRCC [5,16]. The *NRF2* pathway regulates several genes involved in oxidative stress regulation, cell proliferation, and drug metabolism [15]; *NQO1* expression in the *NRF2* pathway is associated with decreased survival [16]. In this study, *NQO1* was identified as an overexpressed DEG, and dysregulation of the *NRF2* pathway by *NQO1* may cause a decrease in survival rate. Downregulated expression of genes involved in insulin-like growth factor-, cell–cell junction-, cell cycle-, inflammatory response-, and steroid synthesis-related pathways, which are associated with *TFE3* fusion, has been confirmed [9,17,18].

Some pathways—GPCR signaling-, development-, axon guidance-, differentiation-, nicotine metabolism-, extracellular matrix-, and integrin-related pathways—were newly to be associated with *TFE3* fusion-positive PRCC. These cancer-related pathways provide novel opportunities for targeted therapies.

Among the DEGs, *FN1* was particularly overexpressed in *TFE3* fusion-positive PRCC. *FN1* plays a major role in cell adhesion, growth, migration, wound healing, and embryonic development [19,20]. High *FN1* expression is associated with RCC aggressiveness and, particularly, early systemic progression in patients with PRCC [21]. In our analysis, *FN1* presented the second-highest expression in *TFE3* fusion-positive cases. In addition, *FN1* was the most extensively involved gene among the DEGs participating in multiple pathways, including the inflammatory response-, development-, axon guidance-, extracellular matrix-, and integrin-related pathway. Therefore, we suggest that *FN1* expression is associated with a poor prognosis of PRCC with *TFE3* fusion and that it could be used as a prognostic biomarker for targeted therapy.

DOI: 10.54254/2753-8818/64/2024.18001

Our study has several limitations. The small number of *TFE3* fusion cases (n = 6) and a single source database could have affected the results owing to high variability. The reliability of the findings of this study can be further improved if the same DEGs and pathways are elucidated in additional studies. Further experimental and clinical trials are required to validate the drug candidates extracted using *in silico* analysis.

5. Conclusion

In conclusion, this study not only depicts the landscape of the overall cell signaling and key genes in *TFE3* fusion-positive RCC, but also provides baseline data that can be used to maximize the opportunities for further preclinical and clinical trials. We introduce putative target drugs that are effective in treating *TFE3* fusion-positive PRCC using a systematic computational approach. We believe that, with further experimental validation and clinical trials, our findings will contribute to the development of precision medicine in novel RCC treatment strategies.

Acknowledgements

This work was supported by the National Research Foundation of Korea (NRF) grant funded by the Korean government (MSIT) (NRF-2020R1C1C1007704 to SA), Seoul National University Bundang Hospital (grant number: 08-2024-03734 to SA), the Korea Health Industry Development Institute (KHIDI) and the Ministry of Health & Welfare, Republic of Korea (grant number: RS-2024-00408936 to JWY), and the VHS Medical Center Research Grant, Republic of Korea (VHSMC24030 to JWY).

References

[1] Steffens, S., Janssen, M., Roos, F. C., Becker, F., Schumacher, S., Seidel, C., Wegener, G., Thuroff, J. W., Hofmann, R., Stockle, M., Siemer, S., Schrader, M., Hartmann, A., Kuczyk, M. A., Junker, K., & Schrader, A. J. (2012). Incidence and long-term prognosis of papillary compared to clear cell renal cell carcinoma--a multicentre study. *Eur J Cancer*, *48*(15), 2347–2352. https://doi.org/10.1016/j.ejca.2012.05.002

[2] Hsieh, J. J., Purdue, M. P., Signoretti, S., Swanton, C., Albiges, L., Schmidinger, M., Heng, D. Y. , Larkin, J., & Ficarra, V. (2017). Renal cell carcinoma. *Nat Rev Dis Primers*, *3*, 17009. https: //doi.org/10.1038/nrdp.2017.9

[3] Cairns, P. (2010). Renal cell carcinoma. *Cancer Biomark*, *9*(1–6), 461–473. https://doi.org/10. 3233/CBM-2011-0176

[4] Ricketts, C. J., De Cubas, A. A., Fan, H., Smith, C. C., Lang, M., Reznik, E., Bowlby, R., Gibb, E. A., Akbani, R., Beroukhim, R., Bottaro, D. P., Choueiri, T. K., Gibbs, R. A., Godwin, A. K., Haake, S., Hakimi, A. A., Henske, E. P., Hsieh, J. J., Ho, T. H., . . . Linehan, W. M. (2018). The Cancer Genome Atlas Comprehensive Molecular Characterization of Renal Cell Carcinoma. *Cell Rep*, *23*(1), 313–326 e315. https://doi.org/10.1016/j.celrep.2018.03.075

[5] Rolley, C., Aubert, C., Baize, N., & Bigot, P. (2018). [Management of metastatic renal cell carcinomass]. *Prog Urol*, *28*(14), 777–782. https://doi.org/10.1016/j.purol.2018.07.280 (Prise en charge des metastases du cancer du rein.)

[6] Al-Maghrabi, J., Mufti, S., & Gomaa, W. (2018). The incidence of renal cell carcinoma associated with Xp11.2 translocation/TFE3 gene fusion in Saudi adult patients with renal cancer: a retrospective tissue microarray analysis. *Pol J Pathol*, *69*(4), 376–383. https://doi.org/10.5114/ pjp.2018.81697

[7] Ge, Y., Lin, X., Zhang, Q., Lin, D., Luo, L., Wang, H., & Li, Z. (2021). Xp11.2 Translocation Renal Cell Carcinoma With TFE3 Rearrangement: Distinct Morphological Features and Prognosis With Different Fusion Partners. *Front Oncol*, *11*, 784993. https://doi.org/10.3389/ fonc.2021.784993

[8] Komai, Y., Fujiwara, M., Fujii, Y., Mukai, H., Yonese, J., Kawakami, S., Yamamoto, S., Migita, T., Ishikawa, Y., Kurata, M., Nakamura, T., & Fukui, I. (2009). Adult Xp11 translocation renal

cell carcinoma diagnosed by cytogenetics and immunohistochemistry. *Clin Cancer Res*, *15*(4), 1170–1176. https://doi.org/10.1158/1078-0432.CCR-08-1183

[9] Kauffman, E. C., Ricketts, C. J., Rais-Bahrami, S., Yang, Y., Merino, M. J., Bottaro, D. P., Srinivasan, R., & Linehan, W. M. (2014). Molecular genetics and cellular features of TFE3 and TFEB fusion kidney cancers. *Nat Rev Urol*, *11*(8), 465–475. https://doi.org/10.1038/nrurol.2014.162

[10] Tannir, N. M., Jonasch, E., Albiges, L., Altinmakas, E., Ng, C. S., Matin, S. F., Wang, X., Qiao, W., Dubauskas Lim, Z., Tamboli, P., Rao, P., Sircar, K., Karam, J. A., McDermott, D. F., Wood, C. G., & Choueiri, T. K. (2016). Everolimus Versus Sunitinib Prospective Evaluation in Metastatic Non-Clear Cell Renal Cell Carcinoma (ESPN): A Randomized Multicenter Phase 2 Trial. *Eur Urol*, *69*(5), 866–874. https://doi.org/10.1016/j.eururo.2015.10.049

[11] Xue, H., Li, J., Xie, H., & Wang, Y. (2018). Review of Drug Repositioning Approaches and Resources. *Int J Biol Sci*, *14*(10), 1232–1244. https://doi.org/10.7150/ijbs.24612

[12] Bushmna, F. (2021). *Bushman group allOnco* Version v5). http://www.bushmanlab.org/links/genelists

[13] Griffith, M., Spies, N. C., Krysiak, K., McMichael, J. F., Coffman, A. C., Danos, A. M., Ainscough, B. J., Ramirez, C. A., Rieke, D. T., Kujan, L., Barnell, E. K., Wagner, A. H., Skidmore, Z. L., Wollam, A., Liu, C. J., Jones, M. R., Bilski, R. L., Lesurf, R., Feng, Y. Y., . . . Griffith, O. L. (2017). CIViC is a community knowledgebase for expert crowdsourcing the clinical interpretation of variants in cancer. *Nat Genet*, *49*(2), 170-174. https://doi.org/10.1038/ng.3774

[14] National Comprehensive Cancer Network. *Kidney Cancer (Version 3.2022)*. Retrieved January 12, 2021 from https://www.nccn.org/guidelines/guidelines-detail?category=1&id=1440

[15] Mir, M. C., Albiges, L., Bex, A., Hora, M., Giannarini, G., Volpe, A., Roupret, M., & Board, E. A. U. S. o. O. U. (2021). Management of Metastatic Nonclear Renal Cell Carcinoma: What Are the Options and Challenges? *Eur Urol Oncol*, *4*(5), 843–850. https://doi.org/10.1016/j.euo.2020.05.010

[16] Cancer Genome Atlas Research, N., Linehan, W. M., Spellman, P. T., Ricketts, C. J., Creighton, C. J., Fei, S. S., Davis, C., Wheeler, D. A., Murray, B. A., Schmidt, L., Vocke, C. D., Peto, M. , Al Mamun, A. A., Shinbrot, E., Sethi, A., Brooks, S., Rathmell, W. K., Brooks, A. N., Hoadley, K. A., . . . Zuna, R. (2016). Comprehensive Molecular Characterization of Papillary Renal-Cell Carcinoma. *N Engl J Med*, *374*(2), 135–145. https://doi.org/10.1056/NEJMoa1505917

[17] Huynh, T. P., Barwe, S. P., Lee, S. J., McSpadden, R., Franco, O. E., Hayward, S. W., Damoiseaux, R., Grubbs, S. S., Petrelli, N. J., & Rajasekaran, A. K. (2015). Glucocorticoids suppress renal cell carcinoma progression by enhancing Na, K-ATPase beta-1 subunit expression. *PLoS One*, *10*(4), e0122442. https://doi.org/10.1371/journal.pone.0122442

[18] Sun, G., Chen, J., Liang, J., Yin, X., Zhang, M., Yao, J., He, N., Armstrong, C. M., Zheng, L., Zhang, X., Zhu, S., Sun, X., Yang, X., Zhao, W., Liao, B., Pan, X., Nie, L., Yang, L., Chen, Y., . . . Zeng, H. (2021). Integrated exome and RNA sequencing of TFE3-translocation renal cell carcinoma. *Nat Commun*, *12*(1), 5262. https://doi.org/10.1038/s41467-021-25618-z

[19] Soikkeli, J., Podlasz, P., Yin, M., Nummela, P., Jahkola, T., Virolainen, S., Krogerus, L., Heikkila, P., von Smitten, K., Saksela, O., & Holtta, E. (2010). Metastatic outgrowth encompasses COL-I, FN1, and POSTN up-regulation and assembly to fibrillar networks regulating cell adhesion, migration, and growth. *Am J Pathol*, *177*(1), 387–403. https://doi.org/10.2353/ajpath.2010.090748

[20] Cai, X., Liu, C., Zhang, T. N., Zhu, Y. W., Dong, X., & Xue, P. (2018). Down-regulation of FN1 inhibits colorectal carcinogenesis by suppressing proliferation, migration, and invasion. *J Cell Biochem*, *119*(6), 4717–4728. https://doi.org/10.1002/jcb.26651

[21] Waalkes, S., Atschekzei, F., Kramer, M. W., Hennenlotter, J., Vetter, G., Becker, J. U., Stenzl, A. , Merseburger, A. S., Schrader, A. J., Kuczyk, M. A., & Serth, J. (2010). Fibronectin 1 mRNA

DOI: 10.54254/2753-8818/64/2024.18001

expression correlates with advanced disease in renal cancer. *BMC Cancer*, *10*, 503. https://doi.org/10.1186/1471-2407-10-503

Appendices

appendix A. Supplementary Figures.

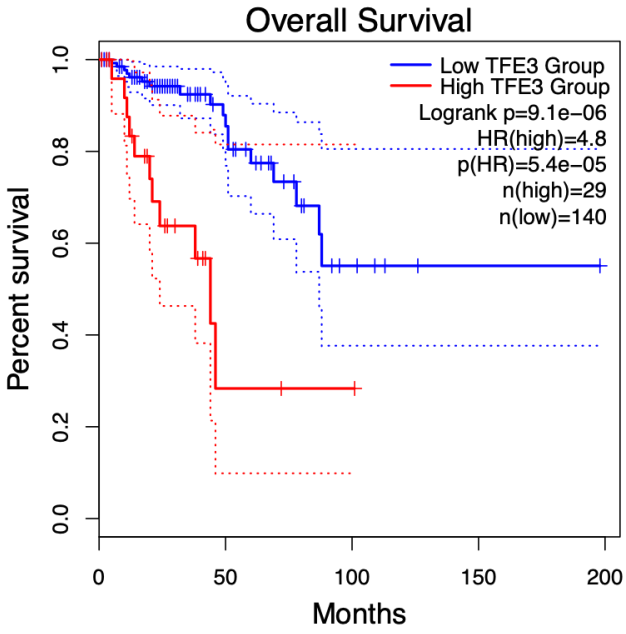

Figure A1. Survival analysis between the *TFE3* high-expression (n = 29) and *TFE3 l*ow-expression group (n = 140).

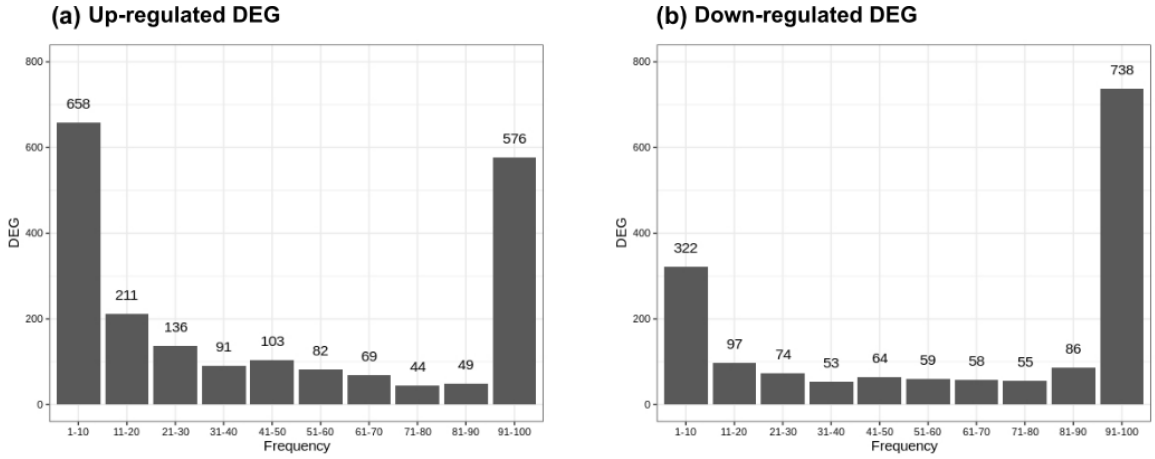

Figure A2. Frequency of differentially expressed genes in 100 iterations.

DOI: 10.54254/2753-8818/64/2024.18001

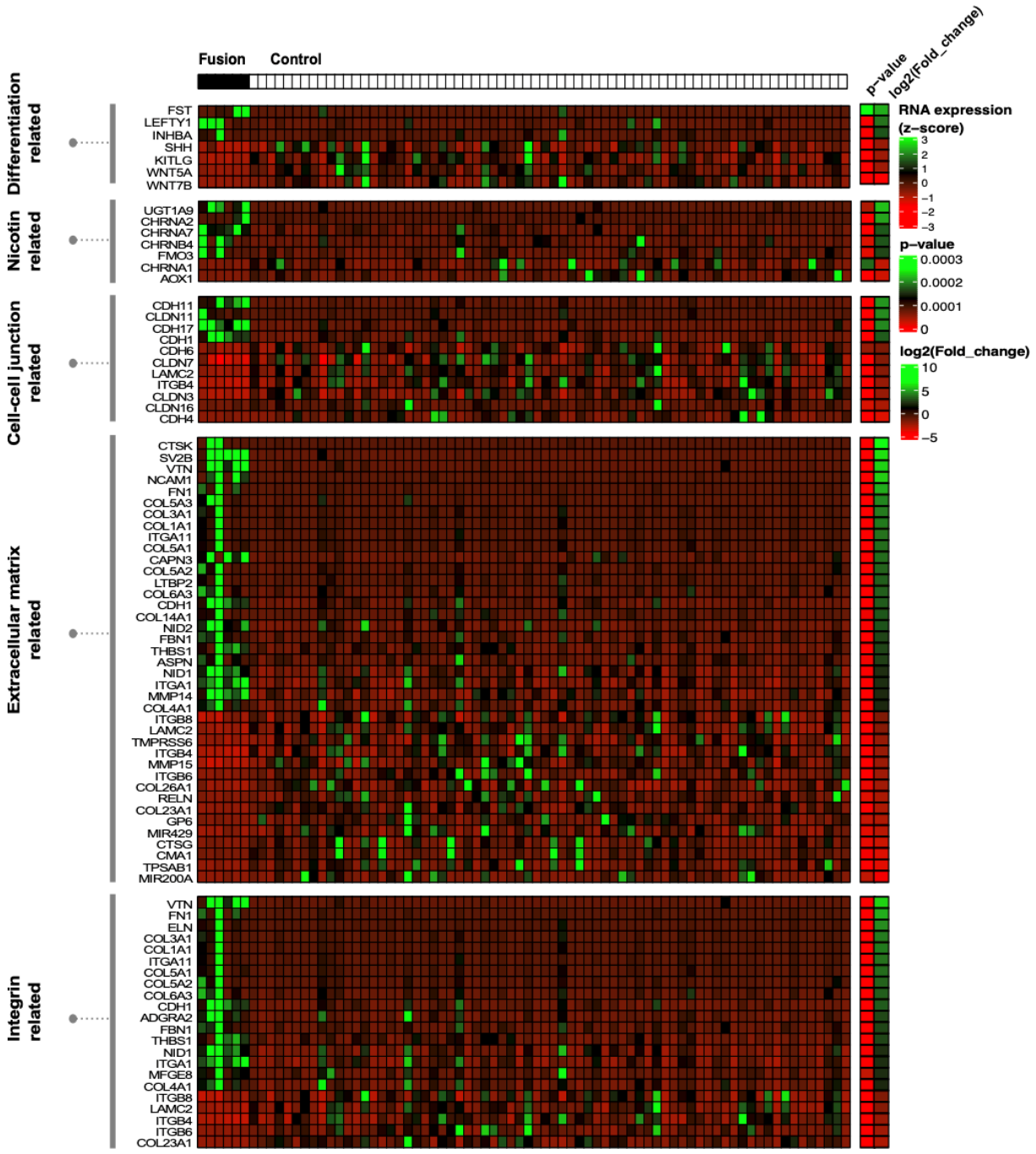

Figure A3. Gene expression heatmap of cancer-related pathways based on the differentially expressed genes.

DOI: 10.54254/2753-8818/64/2024.18001

appendix B. Supplementary Tables.

Table B1. Summary of cancer-related pathways associated with the differentially expressed genes.

Group	Gene	Pathway	Set size	p-value	Source
NRF2-related pathway	*ABCC2, EPHX1, GCLM, GPX3, MAFF, ME1, NQO1, SLC2A14, SLC2A8, SLC5A1, SLC6A1, SLC6A15, SLC6A16, SLC6A18, SLC6A20, SQSTM1, SRXN1, TXNRD1, UGT1A9*	NRF2 pathway	142	< 0.001	Wikipathways
		Photodynamic therapy-induced NFE2L2 (NRF2) survival signaling	23	0.004	Wikipathways
GPCR signaling-related pathway	*ADCY3, CBLC, CD80, DLL1, DRD4, EDN2, EREG, FGF9, GAL, GDF3, GNRH1, IHH, INHBA, INHBE, KITLG, LHB, PRKCG, RGS20, RGS6, SHH, SST, TNFSF10, WNT5A, WNT5B, WNT7B*	GPCR signaling-G alpha i	262	0.003	INOH
		GPCR signaling-pertussis toxin	262	0.003	INOH
		GPCR signaling-G alpha s PKA and ERK	285	0.005	INOH
		GPCR signaling-cholera toxin	270	0.005	INOH
		GPCR signaling-G alpha s Epac and ERK	272	0.005	INOH
		GPCR signaling-G alpha q	274	0.006	INOH
Inflammatory response-related pathway	*CD80, COL1A1, COL3A1, FN1, LAMC2, THBS1, VTN*	Inflammatory response pathway	32	< 0.001	Wikipathways
Development-related pathway	*ADAM23, ANK2, CAMK2A, CD24, CDH4,CHL1, CNKSR1, CNKSR2, COL4A1, COL6A3,DPYSL3, EFNA1, EFNB2, EFNB3, EPHA1, EREG, FGF9, FN1, GAP43, ITGA1, KITLG, KLB, KRT1, KRT15, KRT19, KRT24, KRT27, KRT7, KRT81, KRT86, LEFTY1, LGI3, MYH11, MYL9, NCAM1, NRP2, PKP3, PLXNA4, PPL, RASA4, RASGRF1, SCN2A, SCN4B, SHANK3, SLIT3, SPTA1, SPTBN2, SPTBN5, SRGAP3, ST14, TGM1*	Developmental biology	748	0.006	Reactome

DOI: 10.54254/2753-8818/64/2024.18001

Table B1. (continued)

Insulin-like growth factor-related pathway	*IGF2BP2, IGF2BP3*	Insulin-like growth factor-2 mRNA binding proteins (IGF2BPs/IMPs/VICKZs) bind RNA	3	0.007	Reactome
Axon guidance-related pathway	*ANK2, CAMK2A, CD24, CHL1, CNKSR1, CNKSR2, COL4A1, COL6A3, DPYSL3, EFNA1, EFNB2, EFNB3, EPHA1, EREG, FGF9, FN1, GAP43, ITGA1, KITLG, KLB, MYH11, MYL9, NCAM1, NRP2, PLXNA4, RASA4, RASGRF1, SCN2A, SCN4B, SHANK3, SLIT3, SPTA1, SPTBN2, SPTBN5, SRGAP3*	Axon guidance	487	0.010	Reactome
Steroid synthesis-related pathway	*ADCY3, AKR1C3, CYP17A1, CYP1B1, CYP21A2, CYP7B1, HSD17B6, LHB, LHCGR, NQO1, SCARB1, SULT1E1, UGT1A9*	Steroid hormone biosynthesis—*Homo sapiens* (human)	58	0.006	KEGG
		Ovarian steroidogenesis—*Homo sapiens* (human)	50	0.009	KEGG
		Estrogen metabolism	18	0.009	Wikipathways
		Glucocorticoid biosynthesis	3	0.007	HumanCyc
Cell cycle-related pathway	*CCNB1, RASGRF1, SHH*	Sonic hedgehog receptor ptc1 regulates cell cycle	48	0.007	Wikipathways
Differentiation-related pathway	*FST, INHBA, KITLG, LEFTY1, SHH, WNT5A, WNT7B*	Differentiation pathway	48	0.007	Wikipathways
Nicotine metabolism-related pathway	*AOX1, CHRNA1, CHRNA2, CHRNA7,CHRNB4, FMO3, UGT1A9*	Nicotine metabolism	6	0.002	Wikipathways
		Postsynaptic nicotinic acetylcholine receptors	15	0.005	Reactome
		Activation of nicotinic acetylcholine receptors	15	0.005	Reactome
		Nicotine metabolism pathway	9	0.007	SMPDB
		Highly calcium permeable postsynaptic nicotinic acetylcholine receptors	12	0.002	Reactome

DOI: 10.54254/2753-8818/64/2024.18001

Table B1. (continued)

Cell–cell junction-related pathway	*CDH1, CDH11, CDH17, CDH4, CDH6,CLDN11, CLDN16, CLDN3, CLDN7, ITGB4, LAMC2*	Cell–cell junction organization	62	0.002	Reactome
		Cell junction organization	89	0.003	Reactome
Extracellular matrix-related pathway	*ASPN, CAPN3, CDH1, CMA1, COL14A1, COL1A1, COL23A1, COL26A1, COL3A1, COL4A1, COL5A1, COL5A2, COL5A3, COL6A3, CTSG, CTSK, FBN1, FN1, GP6, ITGA1, ITGA11, ITGB4, ITGB6, ITGB8, LAMC2,LTBP2, MIR200A, MIR429, MMP14, MMP15, NCAM1, NID1, NID2, RELN, SV2B, THBS1,TMPRSS6, TPSAB1, VTN*	miRNA targets in ECM and membrane receptors	42	< 0.001	Wikipathways
		Extracellular matrix organization	295	< 0.001	Reactome
		ECM-receptor interaction - Homo sapiens (human)	82	< 0.001	KEGG
		Degradation of the extracellular matrix	107	< 0.001	Reactome
		Activation of matrix metalloproteinases	31	0.003	Reactome
		Collagen chain trimerization	47	< 0.001	Reactome
		Collagen degradation	36	0.001	Reactome
		Collagen formation	94	0.002	Reactome
		Collagen biosynthesis and modifying enzyme	70	0.002	Reactome
Integrin-related pathway	*ADGRA2, CDH1, COL1A1, COL23A1, COL3A1, COL4A1, COL5A1, COL5A2, COL6A3, ELN, FBN1, FN1, ITGA1, ITGA11, ITGB4, ITGB6, ITGB8, LAMC2, MFGE8, NID1, THBS1, VTN*	β1 integrin cell surface interactions	70	< 0.001	PID
		Integrin cell surface interactions	68	< 0.001	Reactome
		Integrins in angiogenesis	66	0.001	PID
		β5, β6, β7, and β8 integrin cell surface interactions	18	0.001	PID
		Integrin	124	0.006	INOH

Table B2. Differentially expressed genes known to be cancer-related (Bushman group allOnco, http://www.bushmanlab.org/links/genelists). The result (fold changes and p-values) in figure 3 were used. In all cases, $p < 0.001$.

	Gene	**Log_2 (fold change)**
1	*LHCGR*	4.94
2	*FN1*	4.89
3	*FST*	4.89
4	*CDH11*	4.39

DOI: 10.54254/2753-8818/64/2024.18001

Table B2. (continued)

5	*ELN*	4.21
6	*CDH17*	4.12
7	*INHBE*	3.97
8	*COL3A1*	3.84
9	*COL1A*	3.81
10	*MYH11*	3.64
11	*ITGA11*	3.62
12	*ADAM23*	3.46
13	*CDH1*	3.14
14	*GPX3*	3.1
15	*SLIT3*	2.95
16	*CHRNB4*	2.94
17	*NQO1*	2.81
18	*SCARB1*	2.8
19	*RASGRF1*	2.71
20	*THBS1*	2.55
21	*CYP7B1*	2.4
22	*ITGA1*	2.01
23	*AKR1C3*	1.92
24	*MMP14*	1.9
25	*SRXN1*	1.89
26	*CCNB1*	1.65
27	*IGF2BP2*	-1.78
28	*CLDN7*	-2.01
29	*CHL1*	-2.38
30	*TMPRSS6*	-2.41
31	*ITGB4*	-2.45
32	*SRGAP3*	-2.46
33	*SHH*	-2.49
34	*MMP15*	-2.55
35	*TNFSF10*	-2.55
36	*CBLC*	-2.58
37	*KITLG*	-2.62
38	*WNT5A*	-2.63
39	*MIR429*	-3.19

DOI: 10.54254/2753-8818/64/2024.18001

Table B2. (continued)

40	*EPHA1*	-3.83
41	*FGF9*	-4.22
42	*MIR200A*	-4.42
43	*TPK1*	
44	*TYRO3*	
45	*GPC5*	
46	*SOX11*	
47	*ABCB5*	
48	*MAF*	
49	*MST1*	
50	*NEIL1*	
51	*PGGHG*	
52	*CMTM7*	
53	*POU4F1*	
54	*BCL6*	
55	*PPM1E*	
56	*MAL*	
57	*RNASET2*	
58	*BHLHE41*	
59	*PTGIS*	
60	*ALS2CL*	
61	*CR2*	
62	*NLRP2*	
63	*GREM1*	
64	*SLC44A4*	
65	*PLPP3*	
66	*CD109*	
67	*CREB3L1*	
68	*TACSTD2*	
69	*SFRP4*	
70	*MST1R*	
71	*NBL1*	
72	*CD200*	
73	*PADI2*	
74	*FOSL1*	

DOI: 10.54254/2753-8818/64/2024.18001

Table B2. (continued)

75	*ADAM12*
76	*SLC34A2*
77	*PLAG1*
78	*XIRP1*
79	*FOXP3*
80	*TTLL3*
81	*CHN1*
82	*PRLR*
83	*RORC*
84	*PDCD4*
85	*SSTR2*
86	*GRN*
87	*MN1*
88	*KLK4*
89	*NPAP1*
90	*RSPH1*
91	*SYNPO2*
92	*MAMDC4*
93	*CDC25B*
94	*RAC3*
95	*RHOBTB2*
96	*GCNT3*
97	*PLEKHB1*
98	*CST6*
99	*PTGR2*
100	*BUB1*
101	*TK1*
102	*PIM1*
103	*PLCD1*
104	*MUC1*
105	*PAX2*
106	*TP73*
107	*SLC16A1*
108	*GPNMB*
109	*S100A14*

DOI: 10.54254/2753-8818/64/2024.18001

Table B2. (continued)

110	*ABCC11*
111	*SSX2IP*
112	*NR0B1*
113	*SLPI*
114	*PRKN*
115	*SLC19A3*
116	*OSGIN1*
117	*ZMYND10*
118	*CHST11*
119	*TRIB1*
120	*EEF2K*
121	*CASZ1*
122	*CEMIP*
123	*VMP1*
124	*SLC22A3*
125	*SCD*
126	*GLS2*
127	*GREB1*
128	*GSDMB*
129	*INGX*
130	*TRPM8*
131	*NTSR1*
132	*PFKFB2*
133	*SPINK1*
134	*CYP2C8*
135	*CYSLTR2*
136	*RGPD3*